Synthesis and characterisation of SAPO-34 with high surface area

Yadong Bai, Jiajun Zheng, Binbin Fan

School of Chemistry and Chemical Engineering, Taiyuan University of Technology, Taiyuan 030024, People's Republic of China
E-mail: fanbinbin@tyut.edu.cn

Published in Micro & Nano Letters; Received on 15th March 2015; Revised on 20th May 2015; Accepted on 22nd May 2015

SAPO-34 molecular sieve with a high surface area has been successfully synthesised using Y5669 (N-[3-(trimethoxysilyl)propy]aniline) functionalised fumed, silica as the silica source and tetraethylammonium hydroxide as a structure directing agent via a 60-day crystallisation time. X-ray diffraction result indicates that the sample is highly crystalline SAPO-34 and the scanning electron (electron) microscopy images show that the sample is nanosized with a size of ca. 200 nm. N_2 adsorption and ammonia temperature-programmed adsorption results indicate that the synthesised SAPO-34 sample exhibits a much higher microporous area and stronger acidity than the conventional SAPO-34. Moreover, the microporous surface area of the as-obtained SAPO-34 can reach 835 $m^2\ g^{-1}$, which is difficult to realise using other synthesis methods.

1. Introduction: SAPO-34 is a kind of silicoaluminophosphate molecular sieve with a CHA structure [1]. It is composed of a six-membered cyclic cage-shaped crystal grid structure. The diameter of the cycle-shaped mouth of the cage is about 0.40 – 0.45 nm, the structure of which is characterised by an ellipsoid CHA cage with double six-membered cycle, eight-membered cycle and four-membered cycle as well as three-dimensional (3D) cross-channel [2]. SAPO-34 has been considered as a uniquely effective catalyst for the conversion of methanol-to-olefins (MTO) under appropriately mild conditions due to its relatively small pores (0.43 nm), mild acidity and high hydrothermal stability. However, due to fast and strong exothermicity of the MTO reaction, it is often observed that an easy coke formation on SAPO-34 accompanies rapid deactivation and relatively short lifetime, which severely limit its application in industrial field [3, 4].

To solve these problems related to anti-carbon resulting from SAPO-34 microporous structure, scientists have made great efforts [5–14]. On the one hand, the active centre and surface area of SAPO-34 have been increased; on the other hand, hierarchical SAPO-34 has been synthesised. For example, Salmasi *et al.* [15] synthesised SAPO-34 with 677 $m^2\ g^{-1}$ surface area by *in situ* stirring in the process of crystallisation, Nasim *et al.* [16] synthesised hierarchical SAPO-34 with 673 $m^2\ g^{-1}$ surface area by using multiple templates. Furthermore, Wu and Emiel [17] synthesised mesoporous SAPO-34 with 778 $m^2\ g^{-1}$ surface area by the addition of TPOAC into the crystallisation system. However, the surface areas of SAPO-34 molecular sieves in the previously reported literature are below 800 $m^2\ g^{-1}$.

In this Letter, SAPO-34 molecular sieve with a high surface area (863 $m^2\ g^{-1}$) was successfully synthesised by using Y5669 functionalised fumed silica as the silica source and tetraethylammonium hydroxide (TEAOH) as a structure-directing agent via a 60-day crystallisation time, and its textural and acid properties were characterised by X-ray diffraction (XRD), N_2 adsorption, scanning electron microscopy (SEM) and ammonia temperature-programmed adsorption (NH_3-TPD).

2. Experimental

2.1. Synthesis procedure

2.1.1 Functionalisation of fumed silica with Y5669: In a typical functionalisation process, 30 g of fumed silica (Degussa, Aerosil 200) was added into 600 ml of distilled water. The mixture was stirred (100 rpm) under reflux at 373K. Then, 16 ml of Y5669 in methanol solution was added into the former mixture. After reflux for 8 h at 373K, the silica was washed with ethanol several times, then dried at 353K.

2.1.2 Synthesis: The organic functionalised fumed silica was mixed with TEAOH, pseudoboehmite and phosphoric acid, as well as distilled water with a molar composition of 1.0 Al_2O_3: 0.9 P_2O_5: 0.5 SiO_2: 2.0 TEAOH: 60 H_2O, and stirred them at 363K for 24 h. Then, the resulting mixture was hydrothermally treated at 473K in a Teflon-coated stainless-steel autoclave for 60 days. The precipitated product was washed in distilled water, filtered by centrifugation, dried at 373K and calcined in air at 873K. The obtained sample was defined as N-SAPO-34.

For comparison, the conventional SAPO-34 was also prepared by hydrothermal synthesis using TEAOH, boehmite, phosphoric acid, fumed silica and deionised water. Molar ratios of the chemicals were 1.0 Al_2O_3: 0.9 P_2O_5: 0.5 SiO_2:2.0 TEAOH:60 H_2O. Crystallisation was carried out in a Teflon-coated stainless-steel autoclave at 473K for 48 h, and the products were calcined in air at 873K for 6 h. The obtained sample was defined as C-SAPO-34.

2.2. Characterisation: Powder XRD patterns were recorded on a Shimadzu XRD-6000 diffractometer with Cu Kα radiation (40 kV, 30 mA) ($\lambda = 0.1506$ nm). N_2 adsorption/desorption isotherms at 77K were measured on a Quantachrome Autosorb analyser. The surface area was obtained by the Brunauer–Emmett–Teller (BET) equation, whereas the microporous volume and external surface area were calculated by the t-plot method. The pore size distribution was obtained by the adsorption curve based on the density functional theory (DFT) model. Prior to the measurement, samples were outgassed under vacuum for 4 h. The crystal morphology was analysed via SEM (SEM, JMS-6700F). NH_3-TPD was performed on AutochemΠ 2920 TPR/TPD (Micromeritics Instruments). Typically, 10 mg of the sample was pretreated at 400°C in He flow (30 ml min^{-1}) and was subsequently cooled to an adsorption temperature of 120°C. A gas mixture of 5% NH_3/He (V/V) was allowed to make contact with the sample for 30 min at a rate of 30 ml min^{-1}. Subsequently, He flow was passed through the sample to remove weakly adsorbed NH_3 with increasing temperatures of up to 600°C at a rate of 10°C min^{-1}.

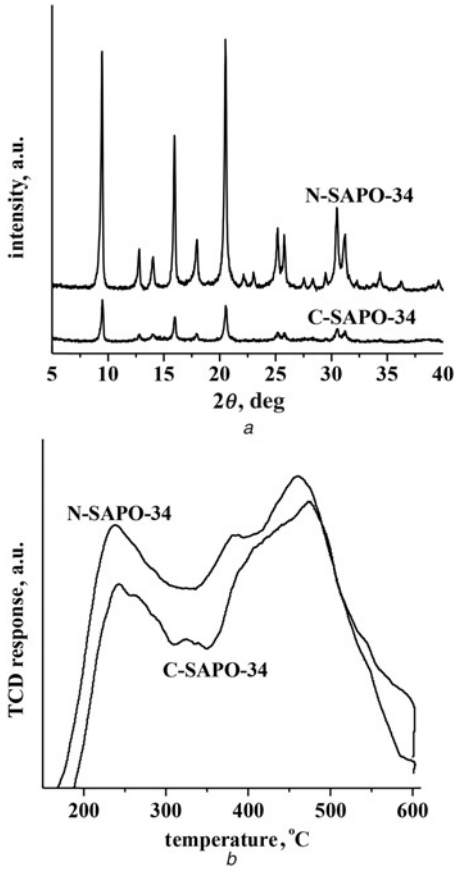

Figure 1 *XRD patterns and NH3-TPD profiles of SAPO-34*
a XRD patterns of SAPO-34
b NH3-TPD profiles of SAPO-34

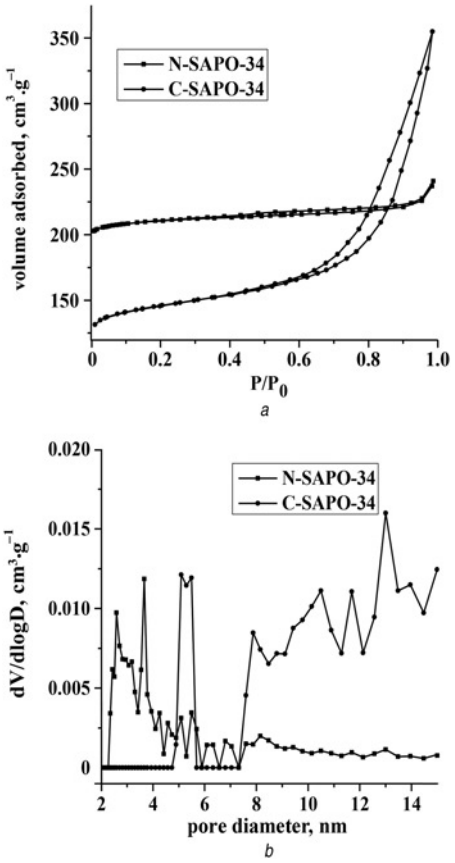

Figure 2 *N_2-adsorption/desorption isotherms and DFT pore distributions of SAPO-34*
a N_2-adsorption/desorption isotherms of SAPO-34
b DFT pore distributions of SAPO-34

3. Results and discussion: Fig. 1*a* shows XRD patterns of SAPO-34 and N-SAPO-34. As can be seen, the N-SAPO-34 and the conventional SAPO-34 both exhibit characteristic diffraction peaks of SAPO-34 (JCPDF47-0429 card) and no other impurity phase was observed. Moreover, the characteristic peak intensity of N-SAPO-34 is much higher than that of C-SAPO-34, suggesting that N-SAPO-34 should have higher crystallinity.

The NH_3-TPD profiles of N-SAPO-34 and C-SAPO-34 are shown in Fig. 1*b*. Two distinctive desorption peaks in the range of 150–300 and 350–600°C are detected for the two samples, which are usually ascribed to ammonia desorption from weak and strong acid sites. For N-SAPO-34, its low-temperature desorption peak is at about 230°C, which is similar to that of C-SAPO-34, but its high-temperature desorption peak at about 460°C is lower than that of C-SAPO-34 by about 30°C. In addition, from the desorption peak areas obtained over the two samples, it can be seen that N-SAPO-34 shows more weak/strong acid amount than C-SAPO-34.

Fig. 2 shows nitrogen adsorption/desorption isotherms and DFT pore distributions of N-SAPO-34 and C-SAPO-34 samples. The N-SAPO-34 sample synthesised with Y5669 functionalised fumed silica as the silica source and at a prolonged crystallisation time is characterised by a type-1 isotherm. This is typical of microporous materials according to the IUPAC classification with a tiny hysteresis loop between 0.4 and 0.9, indicating the presence of certain mesoporosity (Table 1). On the contrary, the C-SAPO-34 sample, synthesised with fumed silica as the silica source and at a short crystallisation time, shows type-IV isotherm and a large hysteresis loop between 0.5 and 0.9, demonstrating the additional presence of obvious mesoporosity in C-SAPO-34. The DFT pore distributions of N-SAPO-34 and C-SAPO-34 are also shown in Fig. 2*b*. It can be clearly seen that the mesopore size in N-SAPO-34 is about 2.2–8 nm and the average pore size is 3.7 nm. By contrast, the mesopore size in C-SAPO-34 is not well-defined and is above 4 nm. Thus, it can be judged that the modified silica source Y5669 can partly increase the medium pore size when it intervenes in the process of crystallisation.

Table 1 summarises the textural properties of the different samples. Compared with C-SAPO-34, N-SAPO-34 shows a much higher mircoporous surface area and volume and lower external surface area and meorporous volume. Notably, its microporous surface area reaches up to 835 $m^2\ g^{-1}$, which is difficult to realise by other synthesis methods. It can be clearly seen that the surface area of N-SAPO-34 increases greatly and the average pore size distribution becomes broader when modified silica source Y5669 participates in the process of crystallisation.

Fig. 3 shows SEM images of the as-obtained SAPO-34 samples. In the case of the C-SAPO-34 sample, the typical cubic-like rhombohedra morphology can be clearly observed. However, there exists the uniformation of the crystal size, which are about

Table 1 Textural properties of the different SAPO-34 samples

Sample	S_{BET}, $m^2\ g^{-1}$	S_{mic}, $m^2\ g^{-1}$	S_{ext}, $m^2\ g^{-1}$	V_{mic}, $cm^3\ g^{-1}$	V_{meso}, $cm^3\ g^{-1}$
N-SAPO-34	862	835	27	0.32	0.11
C-SAPO-34	571	476	95	0.18	0.36

doi: 10.1049/mnl.2015.0101

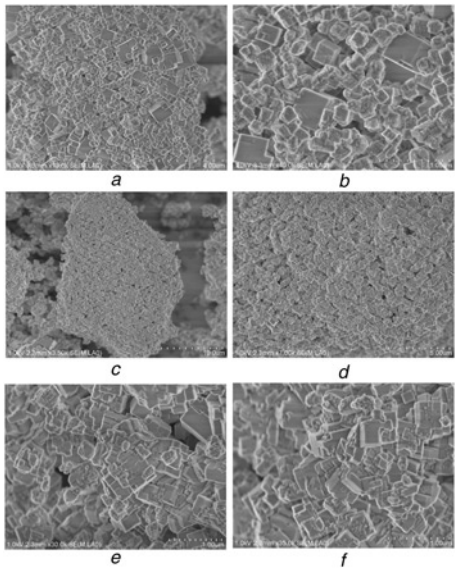

Figure 3 *SEM images of C-SAPO-34 and N-SAPO-34*
a, b C-SAPO-34
c, d, e, f N-SAPO-34

100 nm and around 350 nm. Thus, the N-SAPO-34 shows cubic-like rhombohedra morphology, as does C-SAPO-34, but the crystal size of the former is more uniform than that of the latter.

4. Conclusions: In the hydrothermal system, a SAPO-34 molecular sieve can be successfully synthesised using Y5669 functionalised fumed silica as the silica source and TEAOH as a structure-directing agent when the crystallisation time reaches 60 days. The synthesised SAPO-34 sample is highly crystalline without any impurity phase, and its microporous area can reach up to 835 $m^2 g^{-1}$, which is much larger than that of the conventional SAPO-34 and difficult to realise by using other synthesis methods. Furthermore, compared with the conventional SAPO-34, the synthesised SAPO-34 possesses more acid sites and similar acid strength.

5. Acknowledgments: This work was financially supported by the National Natural Science Foundation of China (nos. 21371129, 21376157 and 21246003), Key Projects in the National Science and Technology Pillar Program during the Twelfth Five-Year Plan Period (no. SQ2011GX04E05929), SinoPEC (no. 111110) and the Natural Science Foundation of Shanxi (no. 2012011005-4).

6 References

[1] Anderson M.W., Sulikowski B., Barrie P.J., Klinowski J.: 'In situ solid-state NMR studies of the catalytic conversion of methanol on the molecular sieve SAPO-34', *J. Phys. Chem.*, 1990, **94**, pp. 2730–2374
[2] Parakash A.M., Unnikrishnan S.: 'Synthesis of SAPO-34: high silicon incorporation in the presence of morpholine as template', *J. Chem. Soc. Faraday Trans.*, 1994, **90**, (15), pp. 2291–2296
[3] Qi G.Z., Xie Z.K., Yang W.M., Zhang S.Q.: 'Behaviors of coke deposition on SAPO-34 catalyst during methanol conversion to light olefins', *Fuel Process. Technol.*, 2007, **88**, pp. 437–441
[4] Liu G.Y., Tian P., Liu Z.M.: 'Modification of SAPO-34 molecular sieve used for methanol to olefins reaction', *Prog. Chem.*, 2010, **22**, pp. 1531–1537
[5] Rustem V., Jorg K., Kanghee C., Minkee C., Ryong R.: 'Dynamics of water diffusion in mesoporous zeolites', *Micropor. Mesopor. Mater.*, 2011, **142**, pp. 236–244
[6] Yang S.T., Kim J.Y., Chae H.J., Kim M., Jeong S.Y., Ahn W.S.: 'Microwave synthesis of mesoporous SAPO-34 with a hierarchical pore structure', *Mater. Res. Bull.*, 2012, **47**, pp. 3888–3892
[7] Sima A., Rouein H., Mahdi N.: 'Statistical analysis of sonochemical synthesis of SAPO-34 nanocrystals using Taguchi experimental design', *Mater. Res. Bull.*, 2013, **48**, (5), pp. 1851–1856
[8] Chen L., Wang R.W., Ding S., *ET AL.*: 'Synthesis and characterization of SAPO-34-H(hierarchical)', *Chem. J. Chin. U*, 2011, **31**, (9), pp. 1693–1696
[9] Arvind K.S., Rekha Y., Ayyamperumal S.: 'Synthesis, characterization, and catalytic application of mesoporous SAPO-34 (MESO-SAPO-34) molecular sieves', *Micropor. Mesopor. Mater.*, 2013, **181**, pp. 166–174
[10] Liu Y.L., Wang L.Z., Zhang J.L.: 'Preparation of floral mesoporous SAPO-34 with the aid of fluoride ion', *Mater. Lett.*, 2011, **65**, pp. 2209–2212
[11] Kim J.Y., Kim J., Yang S.T., Ahn W.S.: 'Mesoporous SAPO-34 with amine-grafting for CO2 capture', *Fuel*, 2013, **108**, pp. 515–520
[12] Duan C., Zhang X., Zhou R., Hua Y., Zhang L.: 'Comparative studies of ethanol to propylene over HZSM-5/SAPO-34 catalysts prepared by hydrothermal synthesis and physical mixture', *Chen J. Fuel Process. Technol.*, 2013, **108**, pp. 31–40
[13] Franz S., Silvia P., Eike B., Stefan K.: 'Carbon templated SAPO-34 with improved adsorption kinetics and catalytic performance in the MTO-reaction', *Micropor. Mesopor. Mater.*, 2012, **164**, pp. 214–221
[14] Wu L.L., Volkan D., Pieter C.M.M.M., Nick J.H.G.M.L., Emiel J.M. H.: 'Mesoporous SSZ-13 zeolite prepared by a dual-template method with improved performance in the methanol-to-olefins reaction', *J. Catal.*, 2013, **298**, pp. 27–40
[15] Salmasi M., Fatemi S., Hashemi S.J.: 'MTO reaction over SAPO-34 catalysts synthesized by combination of TEAOH and morpholine templates and different silica sources', *Sci. Iran.*, 2012, **19**, pp. 1632–1637
[16] Nasim N., Sima A., Rouein H.: 'Hydrothermal synthesis of nanosized SAPO-34 molecular sieves by different combinations of multi templates', *Powder Technol.*, 2014, **254**, pp. 324–330
[17] Wu L.L., Emiel J.M.H.: 'Comparison of mesoporous SSZ-13 and SAPO-34 zeolite catalysts for the methanol-to-olefins reaction', *Catal. Today*, 2014, **235**, pp. 160–168